PNAS RESEARCH ARTICLE | GENETICS

BAP1 is a novel regulator of HIF-1α

Angela Bononi[a,1], Qian Wang[b,c,1], Alicia A. Zolondick[a,d], Fang Bai[b,e,f], Mika Steele-Tanji[a], Joelle S. Suarez[a], Sandra Pastorino[a], Abigail Sipes[a], Valentina Signorato[a], Angelica Ferro[a], Flavia Novelli[a], Jin-Hee Kim[a], Michael Minaai[a,d], Yasutaka Takinishi[a], Laura Pellegrini[a], Andrea Napolitano[a], Ronghui Xu[a], Christine Farrar[a], Chandra Goparaju[a], Cristian Bassi[g], Massimo Negrini[g], Ian Pagano[a], Greg Sakamoto[a], Giovanni Gaudino[a], Harvey I. Pass[h], José N. Onuchic[b,2], Haining Yang[a,2], and Michele Carbone[a,2]

Contributed by José N. Onuchic; received October 18, 2022; accepted December 22, 2022; reviewed by Pier Paolo Pandolfi and I. Le Poole

***BAP1* is a powerful tumor suppressor gene characterized by haplo insufficiency. Individuals carrying germline *BAP1* mutations often develop mesothelioma, an aggressive malignancy of the serosal layers covering the lungs, pericardium, and abdominal cavity. Intriguingly, mesotheliomas developing in carriers of germline *BAP1* mutations are less aggressive, and these patients have significantly improved survival. We investigated the apparent paradox of a tumor suppressor gene that, when mutated, causes less aggressive mesotheliomas. We discovered that mesothelioma biopsies with biallelic *BAP1* mutations showed loss of nuclear HIF-1α staining. We demonstrated that during hypoxia, *BAP1* binds, deubiquitylates, and stabilizes HIF-1α, the master regulator of the hypoxia response and tumor cell invasion. Moreover, primary cells from individuals carrying germline *BAP1* mutations and primary cells in which *BAP1* was silenced using siRNA had reduced HIF-1α protein levels in hypoxia. Computational modeling and co-immunoprecipitation experiments revealed that mutations of *BAP1* residues I675, F678, I679, and L691 -encompassing the C-terminal domain-nuclear localization signal- to A, abolished the interaction with HIF-1α. We found that *BAP1* binds to the N-terminal region of HIF-1α, where HIF-1α binds DNA and dimerizes with HIF-1β forming the heterodimeric transactivating complex HIF. Our data identify *BAP1* as a key positive regulator of HIF-1α in hypoxia. We propose that the significant reduction of HIF-1α activity in mesothelioma cells carrying biallelic *BAP1* mutations, accompanied by the significant reduction of HIF-1α activity in hypoxic tissues containing germline *BAP1* mutations, contributes to the reduced aggressiveness and improved survival of mesotheliomas developing in carriers of germline *BAP1* mutations.**

BAP1 | HIF-1α | hypoxia | mesothelioma | cancer syndrome

BRCA1-associated protein 1 (*BAP1*) is a deubiquitylase that modulates DNA repair by homologous recombination, chromatin assembly, transcription, intracellular calcium (Ca^{2+}) homeostasis, different mechanisms of cell death, and mitochondrial metabolism (1–3). The cells of carriers of heterozygous germline *BAP1* mutations ($BAP1^{+/-}$) contain about 50% of the amount of *BAP1* found in *BAP1* wild-type ($BAP1^{WT}$) individuals, levels that are insufficient for the normal biological activities of *BAP1* (4, 5). $BAP1^{+/-}$ carriers are therefore affected by the *BAP1* cancer syndrome, and close to 100% of them develop one or more cancers during their lifetime (1–3, 6). About 30% of $BAP1^{+/-}$ carriers developed diffuse malignant mesothelioma, a malignancy of the pleura, peritoneum, and/or, rarely, pericardium (1). Germline *BAP1* mutations are transmitted in a Mendelian fashion; hence, multiple cases of mesothelioma are seen in affected families (1, 6–9). The critical causative role of *BAP1* mutations in mesothelioma is underscored by the finding that acquired (somatic) mutations are found in ~ 60% of sporadic mesotheliomas (1, 10). Although mesothelioma can develop in patients affected by other tumor predisposition syndromes caused by inactivating heterozygous germline mutations of *TP53*, *BRCA2*, *BLM*, etc., mesotheliomas in these syndromes are rare (1, 11–14). Instead, 30% of carriers of germline *BAP1* mutations have developed mesothelioma, underscoring the key role of *BAP1* in preventing the malignant transformation of mesothelial cells (1, 6). In addition to mesothelioma, carriers of germline *BAP1* mutations develop other malignancies, among them uveal and cutaneous melanomas, and clear cell renal cell carcinomas (ccRCC) are the most frequent. Indeed, several patients develop multiple malignancies during their life. For a detailed description of the *BAP1* cancer syndrome as well as of the molecular pathways altered by *BAP1* mutations, please see ref. 1. Sporadic mesotheliomas are polyclonal malignancies (15) not linked to germline mutations, mostly caused by exposure to asbestos, and have a dismal median survival of 6 to 24 mo from diagnosis (1, 16–18). Asbestos-induced signature mutations have not been demonstrated in mesothelioma. Mesothelioma is largely resistant to current therapies (16–18). Therapies based on promising experiments in rodents have not been successfully translated to patients (19–23).

Significance

BAP1 modulates crucial cellular pathways that regulate genomic stability and cell death. *BAP1* mutations on the one hand favor malignant transformation and mesothelioma development; on the other hand, they reduce mesothelioma aggressiveness. Investigating this apparent paradox, we discovered that *BAP1* deubiquitylates and stabilizes HIF-1α in hypoxia; thus, *BAP1* inactivating mutations significantly reduce HIF-1α. Given the critical role of HIF-1α in promoting tumor invasion, we propose that: 1) Reduced *BAP1* in the tumor cells and tumor microenvironment of individuals carrying germline *BAP1* mutations may contribute to the reduced invasion and the significantly improved prognosis of mesothelioma; 2) targeting wild-type *BAP1* after tumor development could be a novel effective strategy to reduce HIF-1α protein levels in hypoxic tissues and impair tumor growth.

[1]A.B. and Q.W. contributed equally to this work.

[2]To whom correspondence may be addressed. Email: jose.onuchic@rice.edu, haining@hawaii.edu, or mcarbone@cc.hawaii.edu.

This article contains supporting information online at https://www.pnas.org/lookup/suppl/doi:10.1073/pnas.2217840120/-/DCSupplemental.

Published January 19, 2023.

Therefore, there is an urgent need to identify novel effective therapies (16). Intriguingly, patients with sporadic mesothelioma whose cancer cells carry somatic biallelic *BAP1* mutations may have improved survival of about 1 y compared to mesotheliomas with $BAP1^{WT}$ (24–26). Moreover, when carriers of germline *BAP1* mutations develop mesothelioma, they have a significantly improved median survival of 6 to 7 y; some of them have survived mesothelioma and died of other causes 20+ y later (1, 6, 12, 13, 16, 27, 28). In summary, germline *BAP1* mutations predispose carriers to developing mesothelioma; however, these same mutations, especially when present in both the tumor cells (biallelic mutations) and in the non-malignant cells that include the tumor microenvironment (heterozygous mutations), render mesotheliomas less aggressive and possibly more sensitive to chemotherapy (26). Why? The answer to this question is critical to design novel effective targeted therapies for all mesothelioma patients.

Mesothelioma causes patient demise largely by invading nearby tissues and organs and compromising vital functions; metastases occur late in the course of the disease and are rarely the cause of death (16, 29). Mesotheliomas developing in carriers of germline *BAP1* mutations characteristically grow over the surface of the lungs and nearby organs: invasion is limited and occurs late in the course of the disease (6). Tumor invasion requires that malignant cells acquire the ability to grow in conditions of hypoxia, a process mainly regulated by the hypoxia-inducible factor-1 (HIF-1). The activity of HIF-1 is dependent on a heterodimer formed by an oxygen-dependent α (HIF-1α) subunit, and an oxygen-independent constitutively expressed β subunit (HIF-1β). In normoxia, HIF-1α is targeted by prolyl hydroxylases; once hydroxylated, HIF-1α is recognized by the von-Hippel Lindau E3 ligase (VHL), ubiquitinylated, and targeted for proteasomal degradation. VHL modulates the rapid (~5 min) clearance of HIF-1α in normoxia, while an oxygen-independent slower degradation of HIF-1α further regulates HIF-1α, mainly in hypoxia (30). Hypoxia stabilizes HIF-1α resulting in its nuclear translocation where it forms an active heterodimer with HIF-1β (31). The HIF-1α/HIF-1β dimer (HIF-1) modulates transcription of over 1,000 genes, including anti-apoptotic and pro-angiogenic factors (31) that promote mesothelioma growth (32). As a result of HIF-1 transcriptional activity, cells undergo metabolic reprogramming from oxidative phosphorylation to glycolysis (Warburg effect) and produce biosynthetic intermediates required for the synthesis of NADPH, nucleotides, lipids, and ATP that support tumor cell growth (33, 34). In summary, HIF-1α activity facilitates the invasion of nearby tissues and metastases by allowing cancer cells to grow and survive in a hypoxic environment (34). The oxygen-dependent mechanisms that cause HIF-1α degradation and the genes that suppress HIF-1α in hypoxia have been studied in detail (10, 34), while the gene products that by facilitating HIF-1α expression and activity in hypoxia influence tumor invasion and metastases, remain largely unknown.

We reported that reduced *BAP1* levels increase aerobic glycolysis (5). Because aerobic glycolysis is strongly linked to HIF-1α activation (33, 34), we investigated whether *BAP1* inactivating mutations might induce HIF-1α activity, which in turn promotes glycolysis and tumor cell growth. We found the opposite to be true: $BAP1^{+/-}$ primary cells had reduced HIF-1α levels in hypoxia, and mesothelioma cells carrying biallelic *BAP1* mutations almost constantly lost nuclear HIF-1α. We discovered that *BAP1* binds, deubiquitylates, and stabilizes HIF-1α, an effect best seen in hypoxia. In summary, we discovered that *BAP1* is a critical positive regulator of HIF-1α activity in hypoxia; therefore, when *BAP1* is mutated the levels of HIF-1α are significantly reduced. Our results suggest that the improved prognosis observed in mesotheliomas carrying biallelic *BAP1* mutations, and particularly in those developing in carriers of germline *BAP1* mutations, may be linked to reduced HIF-1α levels in the tumor cells and in the microenvironment.

Results

Reduced *BAP1* Activity Causes Decreased HIF-1α Protein Levels. Immunostaining is considered the most sensitive and specific methodology to detect biallelic *BAP1* mutations, and it is widely used in the differential diagnosis of mesothelioma (10). Nuclear staining is evidence of $BAP1^{WT}$, while the absence of nuclear staining is evidence of mutated, inactive *BAP1* (1, 6, 16, 24, 35). We analyzed *BAP1* and HIF-1α using immunohistochemistry in 49 human mesothelioma biopsies obtained from the National Mesothelioma Virtual Bank (NMVB) (Fig. 1*A*). *BAP1* nuclear staining was present in 14 $BAP1^{WT}$ biopsies and absent in 35 mutated biopsies. HIF-1α nuclear staining was present in 12 (86%) WT biopsies and absent in 26 (74%) mutated biopsies [$\chi^2(1) = 14.7$, $P = 0.0001$] (*SI Appendix*, Fig. S1*A*). In the same biopsies negative for *BAP1* and HIF-1α nuclear staining, the non-malignant nearby mesothelial cells, forming the single cell layer known as "pleura," showed positive nuclear staining for both *BAP1* and HIF-1α (internal positive control) (Fig. 1*A*). These findings suggested that loss of *BAP1* might result in loss of HIF-1α nuclear functions. Additional staining of the only two available mesothelioma biopsies from patients carrying germline *BAP1* mutations revealed the absence of nuclear staining for both *BAP1* and HIF-1α and also reduced to undetectable expression of HIF-1α in the tumor microenvironment compared to tumors with $BAP1^{WT}$ (*SI Appendix*, Fig. S1*B*). Because IHC is not a precise test to quantify differences in protein expression, these findings will need to be validated by Western blot analyses of frozen biopsies of mesotheliomas developing in carriers of germline *BAP1* mutations, which were not available to us.

Because mesothelioma cells carry many gene mutations and gene rearrangements (36) that could influence these results, we studied the possible link between *BAP1* and HIF-1α in primary human mesothelial cells (HM). We incubated primary human mesothelial (HM) cells in 1% oxygen (O_2) for 12 h, which is the hypoxic conditions to induce HIF-1α and found that HM cells transfected with siRNA targeting *BAP1* mRNA (si*BAP1*) contained a significantly reduced amount of HIF-1α protein compared with control HM transfected with scrambled siRNA (Fig. 1 *B* and *C*). Reduced HIF-1α protein levels in *BAP1* silenced HM were reproducibly observed at 3, 6, 12, and 24 h of incubation in 1% O_2 (Fig. 1*D*).

In addition, we observed a direct correlation between reduced *BAP1* and HIF-1α protein levels in primary fibroblast cells we established from skin biopsies from six individuals carrying inherited heterozygous germline *BAP1*-inactivating mutations ($BAP1^{+/-}$), compared to six age- and sex-matched wild-type *BAP1* ($BAP1^{WT}$) control family members, from two separate families: the Wisconsin (W) family and the Louisiana (L) family (4). When incubated in 1% O_2 for 12 h, fibroblasts from $BAP1^{+/-}$ carriers from the W family (Fig. 1*E*) and the L family (Fig. 1*F*) contained significantly less HIF-1α protein compared with their age- and sex-matched $BAP1^{WT}$ controls from the same families, respectively (Fig. 1*G*). This mechanism was not regulated transcriptionally (Fig. 1*H*). Time course experiments in which total cell homogenates and RNAs were collected in parallel after 3, 6, 12, and 24 h of incubation in 1% O_2 confirmed that HIF-1α protein levels were always reduced in fibroblasts from $BAP1^{+/-}$ carriers incubated in 1% O_2 compared to the $BAP1^{WT}$ controls (Fig. 1*I*), while no significant changes were detected in *HIF1A* mRNA levels

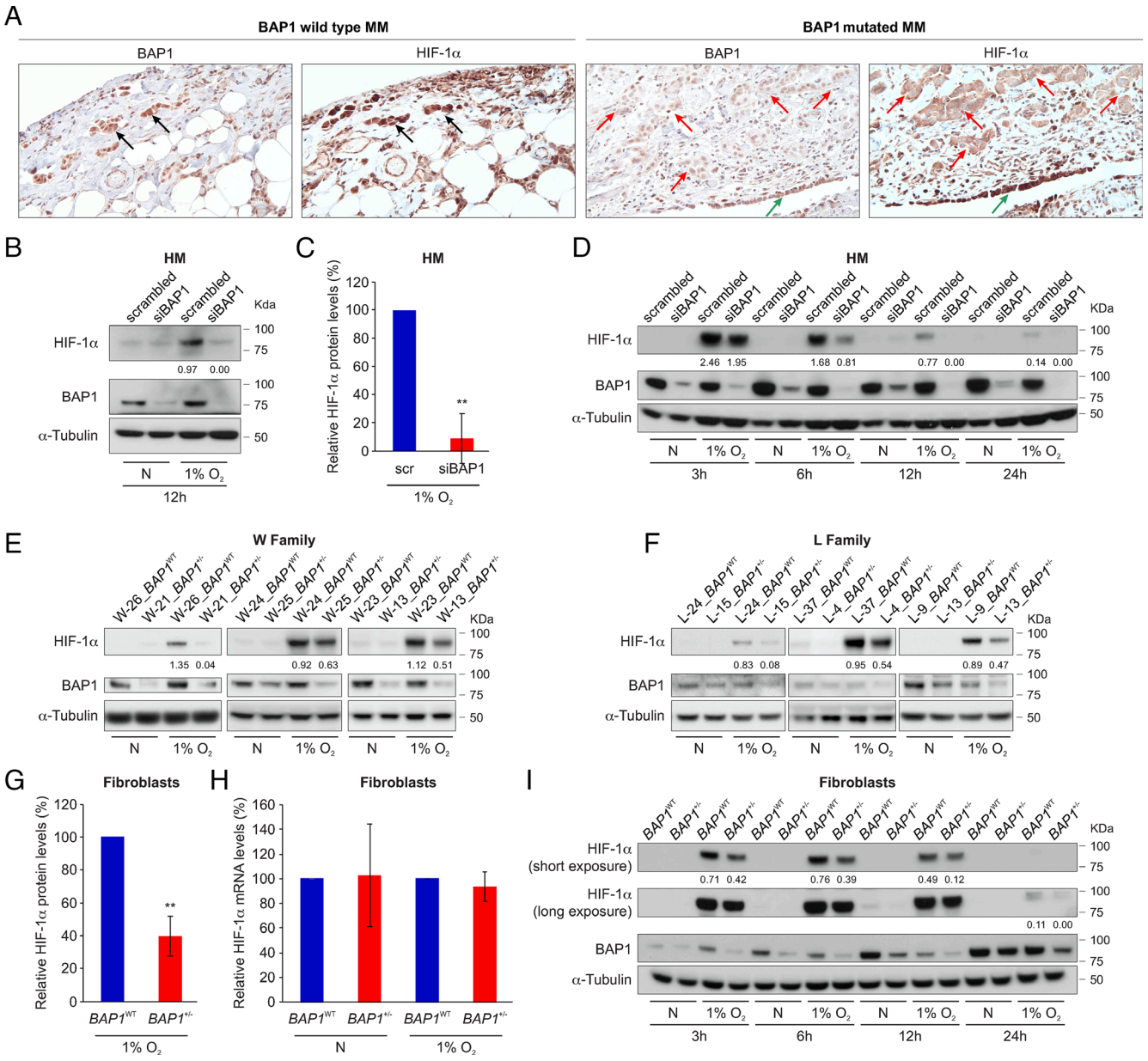

Fig. 1. Reduced *BAP1* protein levels correlate with reduced HIF-1α protein levels. (*A*) Representative HIF-1α immunostaining in human pleural mesothelioma (MM) biopsies. *Left*: Note the nuclear staining for HIF-1α and *BAP1* in *BAP1* WT MM cells infiltrating the chest wall, black arrows. *Right*: Note the absence of HIF-1α and *BAP1* nuclear staining in infiltrating *BAP1*-mutated MM cells, red arrows. Note that the normal nearby mesothelial cells (pleura) retain *BAP1* and HIF-1α nuclear staining, green arrows. Magnification 400×; (Scale bar: 50 μm.) (*B*) Immunoblot, showing that *BAP1* silencing in primary HM cells leads to reduced HIF-1α protein levels after 12 h incubation in 1% O_2. Primary human mesothelial (HM) cells were transfected with control scrambled siRNA or si*BAP1* (a pool of four different siRNAs targeting *BAP1* mRNA: si*BAP1*#1, si*BAP1*#2, si*BAP1*#3 and si*BAP1*#5) and incubated in normoxia (N) or hypoxia (1% O_2) for 12 h. (*C*) Densitometric analysis of HIF-1α protein levels normalized to α-tubulin in *BAP1*-silenced HM relative to scrambled (scr) control (100%); data shown as mean ± SD of n = 4 biological replicates, from four independent experiments. (*D*) Immunoblot: time course showing reduced HIF-1α protein levels in *BAP1*-silenced primary HM incubated in 1% O_2 for the indicated time. (*E* and *F*): Immunoblot: reduced amounts of HIF-1α protein in carriers of germline *BAP1* mutations. Total cell lysates of primary fibroblasts from 6 W (*E*) and 6 L (*F*) family members with or without *BAP1* mutations, matched by gender and age. The W and L families are two families carrying $BAP1^{+/-}$ that we have been studying for ~20 y (8) (*G*) Densitometric analysis of HIF-1α protein levels normalized to α-tubulin from (*E* and *F*); densitometry of bands in $BAP1^{+/-}$ fibroblasts is expressed relative to $BAP1^{WT}$ fibroblasts (100%), matched by gender and age; data shown as mean ± SEM of n = 6 biological replicates per condition, representative of six independent experiments. (*H*) Quantitative PCR analysis of *HIF1A* mRNA expression levels normalized using the geometrical mean of 18S and ACTB reference genes, in $BAP1^{WT}$ and $BAP1^{+/-}$ fibroblasts. mRNA expression levels in $BAP1^{+/-}$ fibroblasts are expressed relative to $BAP1^{WT}$. Data shown as mean ± SD of n = 6 biological replicates per condition, representative of six independent experiments. (*I*) Immunoblot: time course analysis showing reduced HIF-1α levels in $BAP1^{+/-}$ compared to $BAP1^{WT}$ fibroblasts incubated in 1% O_2 for the indicated amount of time. In *B*, *D*, *E*, *F*, and *I*, decimals indicate the amounts of HIF-1α relative to α-tubulin as per densitometry. *P* value calculated using two-tailed unpaired Welch's *t* test, $^{**}P < 0.01$.

(*SI Appendix*, Fig. S1*C*). Reduced HIF-1α protein levels in $BAP1^{+/-}$ carriers were also observed in fibroblasts incubated in 0.1% O_2 for 24 h (*SI Appendix*, Fig. S1*D*). To confirm that *BAP1* regulates HIF-1α, we transduced $BAP1^{+/-}$ fibroblasts with human adenoviruses expressing GFP and $BAP1^{WT}$ for 24 h and cultured these cells in normoxia and in hypoxia for 6 h. Compared to the $BAP1^{+/-}$ fibroblasts transduced with the Ad-GFP control, which maintain about 50% of *BAP1* activity, $BAP1^{+/-}$ fibroblasts transduced with Ad-*BAP1* restored fully functional *BAP1* and these cells displayed similar levels of HIF-1α as those observed in $BAP1^{WT}$ fibroblasts in hypoxia (*SI Appendix*, Fig. S1*E*). Therefore, *BAP1* modulates HIF-1α expression in hypoxia.

BAP1 **Interacts with HIF-1α.** Co-immunoprecipitation (CoIP) and proximity ligation assay (PLA) experiments revealed that 1) HIF-1α and *BAP1* bind to each other and co-precipitate (Fig. 2*A*), and 2) the nuclei of *BAP1*^{WT} cells contained significantly more PLA positive signals—evidence of *BAP1* and HIF-1α interaction—than *BAP1*$^{+/-}$ cells (Fig. 2 *B* and *C*).

We further investigated the specificity of the *BAP1* interaction with HIF-1α in HEK-293 cells expressing Myc-*BAP1* and HA-HIF-1α, using HA-Tag as bait. We found that the Myc-tagged truncated mutant proteins *BAP1*(W) and *BAP1*(L) (8) lose the ability to bind HIF-1α completely (W) or almost completely (L), while the full-length *BAP1* and the catalytically inactive *BAP1* mutant (C91S) (37) interact with HIF-1α (Fig. 2*D*). Deletion fragments of *BAP1* (4) revealed that its C-terminal portion, consisting of the C-terminal domain (CTD) and nuclear localization signal (NLS), is key to the interaction with HIF-1α (Fig. 2*E*). The fragment consisting of the ubiquitin C-terminal hydrolase (UCH) with the non-regular secondary structure (NORS) domains binds to a minor extent (Fig. 2*E*), explaining why the *BAP1*(L) and *BAP1*(W) truncated mutants have lost or have reduced ability to bind HIF-1α, respectively.

We established a computational model of the binding complex of *BAP1* and HIF-1α. The structural predictions of the *BAP1*(CTD-NLS) are highly converged with three different methods: coarse-grained molecular dynamic simulations (38), the I-TASSER web server (39–41) and the RaptorX web server (42) (*SI Appendix*, Fig. S2*A*). For all models, residues 637 to 698 in the CTD form three consecutive helical fragments; in contrast, the full NLS domain is highly disordered (*SI Appendix*, Fig. S2*A*). To study the binding between *BAP1* and HIF-1α, first, a rigid docking protocol was applied to model the binding complex of the CTD of *BAP1* (the NLS domain is removed due to its flexibility) and HIF-1α by using the ClusPro server (43–45) (*SI Appendix*, Fig. S2*B*). We identified residues 1 to 73 of HIF-1α as the main binding interface for *BAP1*. Consistently, RaptorX, a server utilizing co-evolutional information of

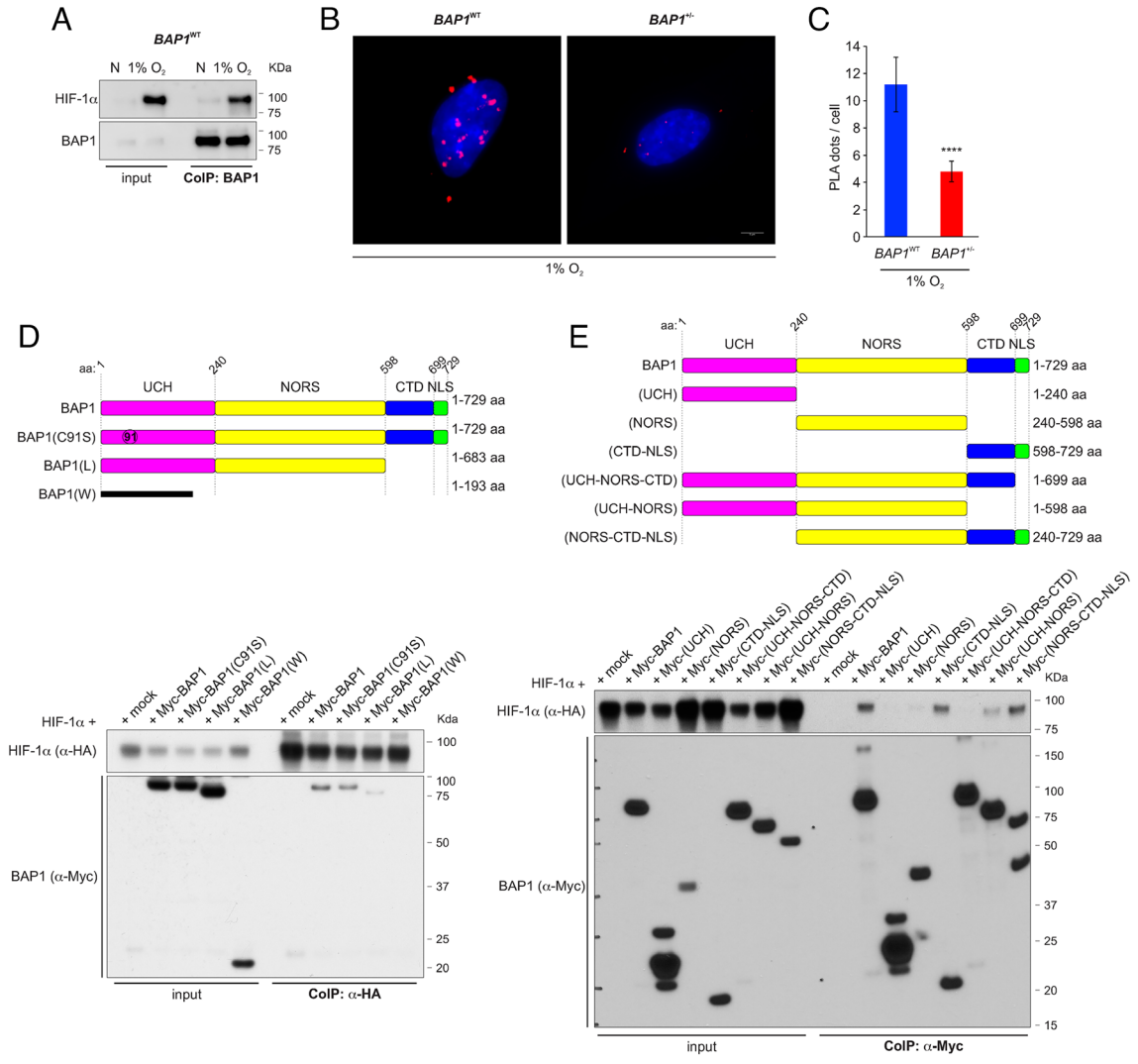

Fig. 2. *BAP1* binds HIF-1α. (*A*) HIF-1α and *BAP1* co-precipitate. CoIP of endogenous HIF-1α and *BAP1*, in *BAP1*^{WT} fibroblasts grown in normoxia (N) or hypoxia (1% O_2) for 4 h, using *BAP1* as a bait. (*B* and *C*) PLA: red dots demonstrate the *BAP1*–HIF-1α interaction in the nuclei of *BAP1*^{WT} and *BAP1*$^{+/-}$ fibroblasts incubated in 1% O_2 for 6 h. Nuclei stained blue with DAPI (*B*); (Scale bar: 5 μm.) Bar graph: quantification of PLA red dots per cell showing reduced *BAP1*–HIF-1α interaction in *BAP1*$^{+/-}$ fibroblasts. Data shown as mean ± SD (n = 20 cells per condition) (*C*). (*D* and *E*) Mapping of the *BAP1*–HIF-1α interaction. The deletion of the CTD-NLS *BAP1* domain –as observed in individuals of the W and L families, greatly reduces the interaction with HIF-1α. (*D*) CoIP of HIF-1α and *BAP1* in homogenates from HEK-293 co-transfected with HA-tagged HIF-1α and Myc-tagged [displayed on top (4)], *BAP1*, catalytic inactive (C91S), L family truncated mutant, W family truncated mutant, using anti-HA resin (*E*) The CTD-NLS domain of *BAP1* is the major contributor to the interaction with HIF-1α, while the fragment consisting of the UCH together with the NORS domains binds to a minor extent. CoIP of HIF-1α and *BAP1* in homogenates from HEK-293 co-transfected with HA-tagged HIF-1α and Myc-tagged *BAP1*, and the Myc-tagged *BAP1* fragments displayed on top (4) using anti-Myc resin.

proteins and deep learning techniques (46), also predicts that residue 1 to 73 of HIF-1α can form contacts with *BAP1* with high probability (*SI Appendix*, Fig. S2*C*). Therefore, we focused on this region (noted as HIF-1α-r73). We used coarse-grained molecular dynamic simulations to model the binding complex of *BAP1* (CTD-NLS) and HIF-1α-r73 (Fig. 3*A*), as well as understanding the binding kinetics (Fig. 3*B*). The NLS domain of *BAP1* binds to HIF-1α-r73 and the thermodynamic stability of the binding complex increases through electrostatic interactions with DNA. Because the NLS domain is highly disordered, it appears as an extended structure and thus greatly increases the searching range of *BAP1* during the binding process. For all simulated trajectories that successfully lead to the correct binding complex, the NLS domain of *BAP1* binds to HIF-1α-r73-DNA ahead of the CTD. This suggests that the binding between *BAP1* and HIF-1α is facilitated by the "fly-casting" mechanism (47, 48). Once the NLS domain of *BAP1* binds to the DNA, it serves as an anchor to increase the local concentration of the CTD of *BAP1* near HIF-1α, which helps the CTD bind sequentially (Fig. 3*B*). Notably, *BAP1* binding to HIF-1α-r73-DNA does not require HIF-1β for the interaction. The critical role of the NLS domain of *BAP1* is supported by the experimental fact that removing this domain greatly decreases the binding to HIF-1α (Fig. 2 *D* and *E*).

CoIP experiments in cells co-transfected with full-length Myc-tagged *BAP1* (Myc-*BAP1*) and HA-tagged full-length HIF-1α, or HIF-1α fragments covering residues 74 to 826 [HIF-1α(74-826)], 2-400 [HIF-1α(2-400)], 401-826 [HIF-1α(401-826)] (Fig. 3*C*), confirmed that *BAP1* binds to the N terminus region of HIF-1α [HIF-1α(2-400)] (Fig. 3*D*). As predicted by our computational model, residues 1 to 73 of HIF-1α are essential for the interaction because HIF-1α(74-826) did not bind *BAP1* (Fig. 3*D*). The binding interfaces between *BAP1*(CTD-NLS) and HIF-1α-r73 in the presence of DNA include three parts: 1) residues K656, R657, K658 and K659 of *BAP1*(CTD-NLS) insert into the major groove of DNA through electrostatic interactions; 2) residues I675, F678, I679 and L691 of *BAP1*(CTD-NLS) form the hydrophobic core with residues F37, L40, Q43, L44 of HIF-1α-r73; 3) the NLS domain of *BAP1* inserts into the major groove of DNA through electrostatic interactions. Among those residues, we found that the ones in *BAP1* are more critical. Mutating those residues to A [*BAP1*(mut)] significantly decreases the binding stability; in contrast, mutating F37, L40, Q43, L44 of HIF1α-r73 to A [HIF1α(mut)] only has a minor effect (*SI Appendix*, Fig. S2*D*).

The accuracy of this model is supported by CoIP experiments revealing that mutations of residues I675, F678, I679, and L691 of *BAP1* (CTD-NLS) to A abolish the interaction with HIF-1α (Fig. 3*E*), while point mutations of residues F37, L40, Q43, L44 of HIF-1α-(r73) to A did not affect the binding with *BAP1* (*SI Appendix*, Fig. S2*E*). All four residues forming the hydrophobic core of *BAP1* must be mutated to completely abolish the binding of HIF-1α, while in the presence of single point mutations *BAP1* interaction with HIF-1α is decreased but not entirely abolished (Fig. 3*F*). We verified that mutating four residues will not significantly change the structure of *BAP1* (CTD-NLS) (*SI Appendix*, Fig. S2*F*). We concluded that the hydrophobic core formed by I675, F678, I679, L691 of *BAP1* and F37, L40, Q43, L44 of HIF1α is sufficient to maintain the binding between the two proteins.

***BAP1* Interacts with HIF-1α and HIF-1β Independently of DNA.** Aligning the crystal structure of HIF-1α-HIF-1β complex (PDB ID: 4zpr) (49) to our structural model for the binding complex of *BAP1*-HIF-1α reveals the significance of residue 1 to 73 of HIF-1α, as this region binds to both *BAP1* and HIF-1β (Fig. 4*A*). Therefore, we checked whether *BAP1* could also bind to HIF-1β. The deletion fragments of *BAP1* (4) revealed that its NORS and CDT-NLS domains are the major contributors to the interaction with HIF-1β (Fig. 4*B*). CoIP experiments in cells co-transfected with full length Myc-tagged *BAP1* (Myc-*BAP1*) and Flag-tagged full-length HIF-1β, or HIF-1β fragments covering residues 2 to 470 [HIF-1β(2-470)], 142-470 [HIF-1β(142-470)], 471-789 [HIF-1β(471-789)], 582-789 [HIF-1β(592-789)] (Fig. 4*C*), showed that *BAP1* binds to the N terminus region of HIF-1β, specifically to the DNA binding and dimerization region [HIF-1β(2-470) and HIF-1β (142-470)] (Fig. 4*D*).

We tested the hypothesis that although DNA facilitates the binding between *BAP1* and HIF-1α, this binding complex still holds in the absence of DNA. Total cell homogenates of cells grown in normoxic or 1% O_2 (hypoxic) conditions were incubated with benzonase for 15, 30, or 60 min, to achieve complete DNA degradation (*SI Appendix*, Fig. S3). Subsequently, endogenous *BAP1* was used as bait to co-immunoprecipitate endogenous HIF-1α and HIF-1β (Fig. 4*E*). These results show that *BAP1* can interact with HIF-1α and HIF-1β even without DNA. The computational analysis of the binding free energy profile between *BAP1* and HIF-1α in the absence of DNA confirmed that the complex of *BAP1*-HIF-1α holds even without DNA, with a binding free energy of ~ 3 kcal/mol (Fig. 4*F*).

Identification of HIF-1α as a Substrate of *BAP1*. It has been reported that the ubiquitin-proteasome pathway regulates the degradation of HIF-1α (51, 52). Since *BAP1* is a member of the UCH subfamily of deubiquitylating enzymes (1), we investigated whether *BAP1* deubiquitylates and stabilizes HIF-1α. We measured the ubiquitylation levels of exogenously expressed HIF-1α in cells co-transfected with HA-tagged ubiquitin (HA-Ub), Flag-HIF-1α and Myc-*BAP1*. CoIP of Flag-HIF-1α showed reduced ubiquitin levels when cells overexpressed *BAP1*, but not in cells overexpressing the catalytic inactive *BAP1*(C91S), compared to mock control (Fig. 5*A*). In vitro de-ubiquitylation assays using purified recombinant proteins confirmed increased deubiquitylation of HIF-1α in the presence of *BAP1*, while in the presence of *BAP1*(C91S), *BAP1*(L), and *BAP1*(W) HIF-1α deubiquitylation was comparable to mock control (Fig. 5*B*). Together, these results demonstrated that *BAP1* deubiquitylates and thus stabilizes HIF-1α.

Discussion

We discovered that *BAP1* binds and deubiquitylates HIF-1α, contributing to the high levels of HIF-1α in hypoxia (Figs. 1–5). Accordingly, primary cells we derived from carriers of germline heterozygous *BAP1* mutations, as well as cells in which we down-regulated *BAP1* using siRNA, and mesothelioma biopsies containing tumor cells with biallelic *BAP1* inactivation, displayed significantly reduced levels of HIF-1α and loss of nuclear HIF-1α compared to normal cells or tumor cells with $BAP1^{WT}$ (Fig. 1). Therefore, our data suggest that *BAP1* is a key regulator of HIF-1α and its tumor-promoting activities. In previous studies performed in normoxic conditions, we demonstrated that *BAP1* regulates intracellular Ca^{2+} flux by binding and deubiquitylating, and thus stabilizing the IP3R3 receptor (4). Therefore, *BAP1* deubiquitylating activity appears to remain active in both conditions, normoxia and hypoxia.

We found that *BAP1* also binds to the N terminus region of HIF-1β, specifically to the DNA binding and dimerization region

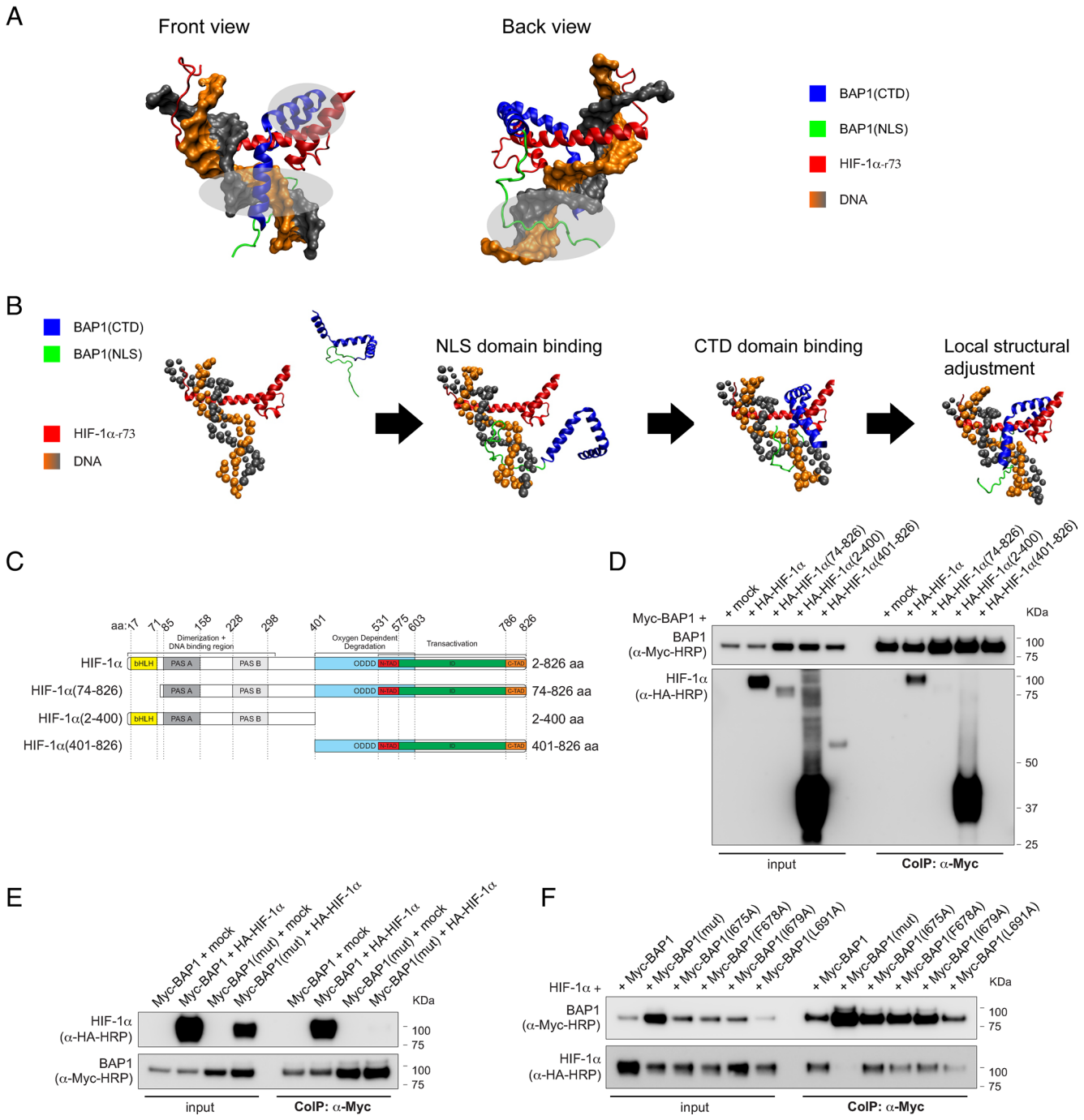

Fig. 3. The CDT-NLS domain of *BAP1* interacts with residues 1 to 73 of HIF-1α. (*A*) Structural modeling for the binding complex of *BAP1*(CTD-NLS) and HIF-1α (1-73) (residues 1 to 73 of HIF-1α) in the presence of DNA. The CTD of *BAP1* is colored in blue, the NLS domain of *BAP1* is colored in green, HIF-1α is colored in red, DNA is colored in orange and grey; three interacting regions are marked by light silver circles. (*B*) Coarse-grained molecular dynamic simulations to model the binding complex of *BAP1*(CTD-NLS) and HIF-1(1-73). The NLS domain (colored in green) is extended to increase the searching range of *BAP1* to bind to HIF-1α. The NLS domain of *BAP1* binds to HIF-1α first. Then the CTD binds sequentially. (*C*) HA-tagged HIF-1α fragments and HIF-1α domains: basic-helix-loop-helix motif (bHLH) protein, two Per and Sim (PAS) domain (*A* and *B*), oxygen-dependent degradation domain (ODDD), two transactivation domains (TAD): NH2-terminal (N-TAD) and COOH-terminal (C-TAD), intervening inhibitory domain (ID). (*D*) *BAP1* binds to the N terminus region of HIF-1α [HIF-1α(2-400)]. Residues 1 to 73 of HIF-1α are essential for the interaction because HIF-1α(74-826) did not bind *BAP1*. CoIP of *BAP1* and HIF-1α in homogenates from HEK-293 co-transfected with Myc-*BAP1* and HA-tagged HIF-1α or the HA-tagged HIF-1α fragments displayed in (*C*), or the empty vector (mock); anti-Myc resin was used as bait. (*E*) Point Mutations of residues I675, F678, I679, and L691 of *BAP1* abolish the interaction with HIF-1α. CoIP of *BAP1* and HIF-1α in homogenates from HEK-293 co-transfected with Myc-*BAP1* or Myc-*BAP1*(mut) (in which residues I675, F678, I679, L691 of *BAP1* are mutated to Alanine), and HA-tagged HIF-1α or empty vector (mock); anti-Myc resin was used as bait. (*F*) The simultaneous mutation of residues I675, F678, I679, L691 of *BAP1* abolish the interaction with HIF-1α, while single-point mutations decrease but do not abolish this interaction. CoIP of *BAP1* and HIF-1α in homogenates from HEK-293 co-transfected with HA-tagged HIF-1α and Myc-*BAP1*, or Myc-*BAP1*(mut) (in which residues I675, F678, I679, L691 of *BAP1* are mutated to Alanine), or Myc-*BAP1* mutants carrying each individual point mutation; anti-Myc resin was used as bait.

(Fig. 4). The crystal structure of HIF-1α-HIF-1β complex (PDB ID: 4zpr) (49) shows that without *BAP1*, HIF-1α, and HIF-1β bind to DNA (49), thus *BAP1* is not required for HIF-1α-HIF-1β complex formation. Aligning the crystal structure of HIF-1α-HIF-1β complex (PDB ID: 4zpr) (49) to our structural model for the binding complex of *BAP1*-HIF-1α showed that both *BAP1* and HIF-1β bind to the

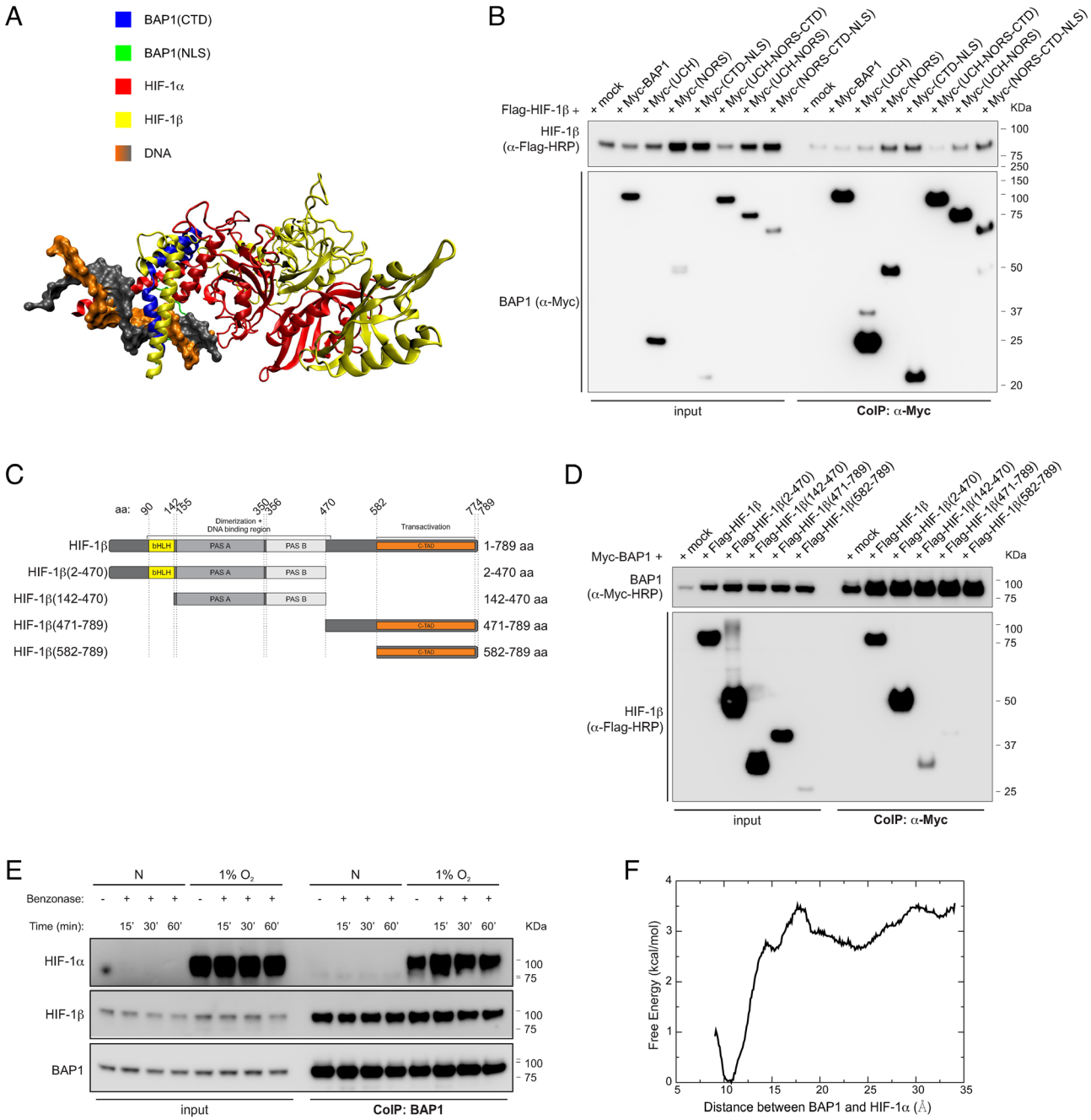

Fig. 4. *BAP1* binding to HIF-1α and HIF-1β does not require DNA. (*A*) Shared binding region among *BAP1*, HIF-1α, and HIF-1β. The CTD of *BAP1* is colored in blue, the NLS domain of *BAP1* is colored in green, HIF-1α is colored in red, DNA is colored in orange and grey, and HIF-1β (colored in yellow) is docked onto the binding complex of *BAP1* and HIF-1α by utilizing the crystal structure of HIF-1α–HIF-1β (PDB ID: 4zpr) (49). Missing residues of the crystal structure are added by the SWISS-MODEL server (50). (*B*) HIF-1β interacts with the NORS and CTD-NLS domain of *BAP1*. CoIP of HIF-1β and *BAP1* in homogenates from HEK-293 co-transfected with Flag-tagged HIF-1β and Myc-tagged *BAP1* and the Myc-tagged *BAP1* fragments displayed in Fig. 2*E* (4), using anti-Myc resin. (*C*) Flag-tagged HIF-1β fragments and HIF-1β domains: basic-helix-loop-helix motif (bHLH) protein, two Per and Sim (PAS) domain (*A* and *B*), and COOH-terminal transactivation domain (C-TAD). (*D*) CoIP of *BAP1* and HIF-1β in homogenates from HEK-293 co-transfected with Myc-*BAP1* and Flag-HIF-1β or the Flag-HIF-1β fragments displayed in (*C*), or the empty vector (mock); anti-Myc resin was used as bait. (*E*) HEK-293 cells were grown in normoxia (N) or hypoxia (1% O_2) for 4 h. Cell homogenates were collected, treated with benzonase for 15, 30 or 60 min (*SI Appendix*, Fig. S3), and then used to co-immunoprecipitate endogenous HIF-1α and HIF-1β using *BAP1* as bait. (*F*) Computational binding free energy profile between *BAP1* and HIF-1α in the absence of DNA; the result indicates that the binding complex formed by *BAP1* and HIF-1α can still hold when DNA is absent (the binding free energy ~ 3 kcal/mol).

same residues of HIF-1α (1-73) on the DNA; however, in Fig. 3*B*, we demonstrate that *BAP1*, HIF-1α and the DNA form a complex without HIF-1β. In addition, we show that after total degradation of DNA, *BAP1* remains bound to both HIF-1α and HIF-1β (Fig. 4*A*). Therefore, our data indicate that *BAP1* is not required for HIF-1α-HIF-1β complex formation to functionally bind to DNA, that HIF-1β is not required for *BAP1*-HIF-1α complex formation to functional binding to DNA, and that although DNA facilitates the binding of *BAP1* and HIF-1α, it is not required to maintain the binding of both *BAP1*-HIF-1α and *BAP1*-HIF-1β.

In summary, our data suggest that *BAP1* directly binds and stabilizes both HIF-1α and HIF-1β increasing their intra-nuclear availability for dimer formation, thus fine-tuning HIF activities required to support malignant cell growth. So far, the pathogenic variants reported in ClinVar for both HIF-1α and HIF-1β are not located among the crucial residues of HIF-1α-r73 where HIF-1α

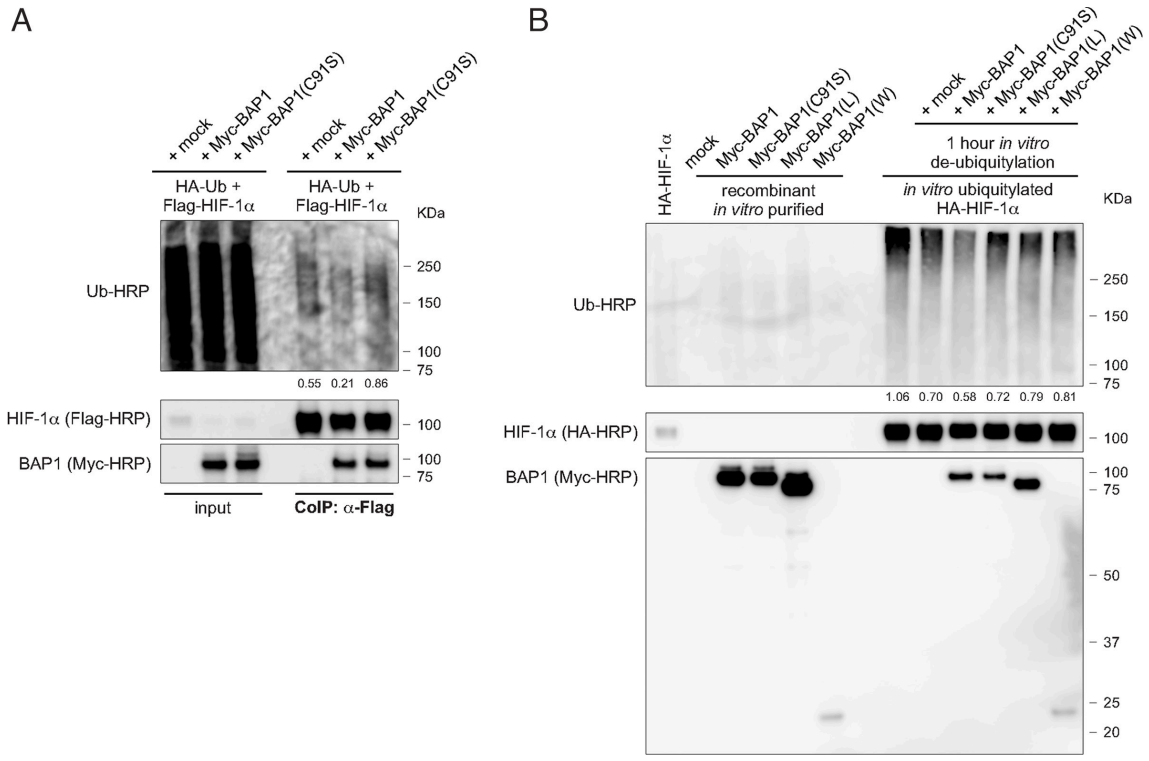

Fig. 5. *BAP1* Deubiquitylates HIF-1α. (*A*) Reduced endogenous ubiquitylation of HIF-1α in HEK-293 cells co-transfected with Flag-tagged HIF-1α and Myc-tagged *BAP1*, catalytic inactive (C91S), or mock. Cells were treated with 10 μM MG-132 for 3 h, then total cell homogenates were collected and HIF-1α immunoprecipitated using anti-Flag resin. Ubiquitylation levels of the immunocomplexes were detected using an anti-Ub-HRP antibody and normalized on the total amount of Flag-HIF-1α immunoprecipitated (decimals indicate the ratio as per densitometric analysis). (*B*) Western blot analysis of in vitro ubiquitylation/de-ubiquitylation assay. HA-HIF-1α ubiquitylated in vitro, and subsequently incubated with immunopurified Myc-*BAP1*, Myc-*BAP1*(C91S), Myc-*BAP1*(L), Myc-*BAP1*(W), or mock, for 1 h. Ubiquitylation levels were detected using an anti-Ub-HRP antibody and normalized on the total amount of HA-HIF-1α (decimals indicate the ratio as per densitometric analysis).

can bind to *BAP1*, HIF-1β and DNA, or of HIF-1β (2-470) where HIF-1β can bind to *BAP1*, HIF-1α, and DNA. This finding suggests that tumor cell clones that may acquire HIF-1α and/or HIF-1β mutations that impair their binding to *BAP1* may be negatively selected compared to tumor cell clones expressing HIF-1α and HIF-1β that maintain the capacity to bind to *BAP1*.

HIF-1α is the master regulator of cell growth in hypoxia (33, 34). HIF1 activity is regulated by the interaction of HIF-1α with >100 other proteins (53). Among them, VHL plays a key role by recruiting an E3-ubiquitin ligase complex to mediate HIF-1α protein degradation in normoxia. Biallelic *BAP1* mutations occur in several human cancers (1); their tumor cells, based on our data studying mesothelioma, should contain reduced HIF-1α levels. However, this might not remain true in malignancies in which the *VHL* gene (34)—or other genes that suppress HIF-1α (10)—are also mutated and thus display constitutively high levels of HIF-1α, which may overrun the fine-tuning *BAP1* deubiquitylating activity.

In addition to VHL, which is active in normoxia, other proteins mediate the ubiquitylation of HIF-1α in hypoxia. The UCH-L1 (UCHL1) is a deubiquitylase that has been shown to positively modulate HIF-1α levels (54). Our data identified *BAP1* as a deubiquitylase that binds and inhibits the degradation of HIF-1α, an effect best observed in hypoxia. *BAP1* shares 23% sequence homology with UCHL1 (55). UCHL1 hydrolyzes the C-terminal peptide tails of small ubiquitin derivatives but cannot hydrolyze large ubiquitin chains because of short active site crossover loops. *BAP1* instead has long crossover loops and thus can process polyubiquitin chains (55, 56). Thus, UCHL1 and *BAP1* are both independently required for HIF-1α stabilization and activities. UCHL1 and *BAP1* were both identified as deubiquitylases for γ-tubulin through screening a siRNA library of deubiquitylases; however, when both UCHL1 and *BAP1* were depleted using siRNA, the degradation of γ-tubulin was comparable to the γ-tubulin levels after either *BAP1* or UCHL1 silencing alone (57). Future studies shall address whether these two ubiquitin hydrolases interact in modulating HIF-1α levels in hypoxia and whether their effects are cell type specific.

It has been proposed that targeting UCHL1 might reduce HIF-1α stabilization and impair tumor growth (54). Our data point to *BAP1* as a novel target to reduce HIF-1α tumor-promoting activity in malignancies with elevated HIF-1α levels and intact VHL. We identified the nucleotides responsible for the binding between *BAP1* and HIF-1α and *BAP1* and HIF-1β. Previous studies using the HIF-1α inhibitor YC-1 (58) or siRNAs targeting HIF-1α in mesothelioma cells in tissue culture (59), revealed increased apoptosis; however, the authors suggested that an additional blockade was required to inhibit growth signals completely. We are designing small molecules to test the hypothesis that their intra-pleural administration alone or together with HIF-1α inhibitors, will interfere with the binding among *BAP1* and HIF-1α and cause HIF-1α degradation. It is hoped that reduced HIF-1α activity will impair mesothelioma growth and increase susceptibility to therapy, as observed in patients carrying germline *BAP1* mutations and tumors with biallelic *BAP1* inactivating mutations (6).

Mesotheliomas have large areas of hypoxia (60). The activity of HIF-1α-induced metabolic reprogramming provides malignant cells with maximal growth support in a hypoxic tumor microenvironment. Therefore, the reduced levels of HIF-1α in *BAP1*-mutated tumor cells may contribute to the reduced tumor aggressiveness of *BAP1*-mutant mesotheliomas, compared to mesotheliomas with $BAP1^{WT}$ (6, 12, 13, 27, 28). Mesotheliomas developing in carriers of germline *BAP1* mutations invariably carry biallelic inactivating *BAP1* mutations ($BAP1^{-/-}$), easily detectable by the absence of nuclear *BAP1*

staining, while the cells forming the tumor microenvironment carry heterozygous germline *BAP1* mutations (*BAP1*$^{+/-}$) (1, 8, 14). About ~60% of sporadic mesotheliomas carry somatic (acquired) biallelic inactivating *BAP1*$^{-/-}$; however, the cells forming the tumor microenvironment are *BAP1*^{WT} (1, 8, 14). Our hypothesis is that in sporadic *BAP1*$^{-/-}$ mesotheliomas, *BAP1* loss results in reduced HIF-1α in the malignant cells; however, the surrounding hypoxic tumor cell microenvironment comprised of *BAP1*^{WT} cells will maintain stable HIF-1α levels that sustain tumor cell invasion. Conversely, the hypoxic tumor microenvironment of mesotheliomas developing in patients carrying germline *BAP1* mutations express reduced HIF-1α. Accordingly, these patients have less invasive tumors. This hypothesis, based on our in vitro experiments (Fig. 1 *E–I*), was supported by IHC analyses in which we studied mesothelioma biopsies from patients carrying germline *BAP1* mutations. In their mesothelioma biopsies, IHC showed undetectable HIF-1α expression in the tumor cells and reduced HIF-1α expression in the cells forming the tumor microenvironment (*SI Appendix*, Fig. S1*B*), compared to sporadic *BAP1*$^{-/-}$ mesothelioma biopsies which maintained HIF-1α expression in the surround *BAP1*^{WT} cells (Fig. 1*A*). Altogether, these data suggest that reduced HIF-1α levels may contribute to the reduced aggressiveness of mesothelioma in carriers of germline *BAP1* mutations (6, 12, 13, 27, 28). Reduced HIF-1α levels may also render mesothelioma cells more susceptible to cell death in hypoxia and this could contribute to the reported increased response to chemotherapy of *BAP1* mutated mesotheliomas (26), and in those that develop among carriers of germline *BAP1* mutations, in particular (6).

BAP1 mutations are not associated with an improved prognosis in uveal melanoma (UVM) and ccRCC, the other two malignancies that, together with mesothelioma, most often carry *BAP1* mutations (1). Moreover, the loss of *BAP1* expression has been detected together with increased expression of HIF-1α in UVM (61) and ccRCC (62, 63). These results appear to contradict our findings. However, in about 90% of ccRCC, the initiating event is the inactivation of the *VHL* gene located on chromosome 3 (64). Physiologically, VHL binds to HIF-1α targeting it for ubiquitylation and proteasomal degradation, therefore, once *VHL* is lost, HIF-1α ubiquitylation is markedly reduced, and its levels are significantly increased (33, 34) an effect that should render the reduced deubiquitylation of HIF-1α by *BAP1* in *BAP1* deficient cells physiologically less relevant. The study in UVM (61) measured *HIF1A* mRNA levels and their relationship to *BAP1* transcription. Here we report that *BAP1* modulates the stability of the HIF-1α protein and that it does not regulate HIF-1α gene transcription. Moreover, similarly to ccRCC, deletions of chromosome 3 are frequent in UVM (65) with subsequent loss of VHL. In mesothelioma, instead, nucleotide level deletions as well as minute deletions of 100 to 300 bp are frequent throughout the *BAP1* gene located on chromosome 3p, and nearby *SETD2*, *SMARCC1*, *PBRM1* genes, but deletions extending to the *VHL* gene are very rare (66). Therefore, the effects of reduced deubiquitylating activity of *BAP1* mutations on the HIF-1α protein may be more relevant in mesothelioma compared to ccRCC and UVM in which the very frequent inactivation of VHL may result in elevated levels of HIF-1α independently from *BAP1* deubiquitylating activity. Overall, our findings may help explain the opposite effects on survival in *BAP1*-mutated mesothelioma compared to *BAP1*-mutated ccRCC and UVM. Further studies in renal cell carcinomas and UVMs, compared to mesothelioma, are necessary to fully address the mechanisms and the possible relationship with HIF-1α expression in these malignancies.

In summary, we report that *BAP1* deubiquitylates and thus stabilizes HIF-1α in hypoxia, and, therefore, *BAP1* mutations significantly reduce HIF-1α protein levels. Given the well-established role of HIF-1α in promoting tumor growth in hypoxia, we propose that the reduced aggressiveness and improved prognosis of mesothelioma in carriers of germline *BAP1* mutations may result, at least in part, from the combined reduced HIF-1 activity caused by biallelic *BAP1* mutations in mesothelioma cells and the presence of heterozygous *BAP1* mutations in the cells that form the tumor microenvironment.

Materials and Methods

Subjects. *BAP1*$^{+/-}$ mutant carriers and unaffected controls were recruited from the L and W families and provided informed written consent allowing their specimens to be used for this project. The collection and use of patient information and samples were approved by the Institutional Review Board (IRB) of the University of Hawaii (IRB no. CHS14406).

Technical Procedures. Cell cultures, immunohistochemistry, gene silencing, qPCR, western blot (WB), Co-IP, in vitro ubiquitylation and de-ubiquitylation assays, Duolink PLA, and computational modeling were performed according to standard techniques and are described in *SI Appendix*.

Statistics and Reproducibility. *P* values were calculated using two-tailed unpaired Welch's *t* test, unless otherwise specified. *P* values < 0.05 were considered statistically significant and marked with asterisks ($*P < 0.05$; $**P < 0.01$; $***P < 0.001$; $****P < 0.0001$), as indicated in the figure legends. All data collected met the normal distributions assumption of the test. Data are represented as mean ± SD, unless otherwise specified in the figure legends. The exact sample size (n) for experimental groups/conditions and whether samples represent technical or cell culture replicates are indicated in the figure legends. The results shown are representative of experiments independently conducted three times that produced similar results.

Data, Materials, and Software Availability. All study data are included in the article and/or *SI Appendix*.

ACKNOWLEDGMENTS. We are in debt to the patients who donated their specimens for research. We would like to acknowledge the UH Cancer Center Microscopy, Imaging, and Flow Cytometry Core and the Leica Thunder Live Cell 3D microscope SIG: NIH S10OD0028515-01 for supporting this work. We acknowledge the NMVB for providing the mesothelioma biopsies. M.C. and H.Y. have a patent issued for "Using Anti-HMGB1 Monoclonal Antibody or other HMGB1 Antibodies as a Novel Mesothelioma Therapeutic Strategy" and a patent issued for "HMGB1 As a Biomarker for Asbestos Exposure and Mesothelioma Early Detection." M.C. and H.Y. report funding from the National Institute of Environmental Health Sciences (NIEHS) 1R01ES030948-01 (M.C. and H.Y.), the National Cancer Institute (NCI) 1R01CA237235-01A1 (M.C. and H.Y.) and 1R01CA198138 (M.C.), the US Department of Defense (DoD) W81XWH-16-1-0440 (H.Y., M.C., and H.I.P.), and from the UH Foundation through donations from the Riviera United-4-a Cure (M.C. and H.Y.), the Melohn Family Endowment, the Honeywell International Inc., the Germaine Hope Brennan Foundation, and the Maurice and Joanna Sullivan Family Foundation (M.C.). H.I.P. and H.Y. report funding from the Early Detection Research Network NCI 5U01CA214195-04. H.I.P. reports funding from Genentech, Belluck, and Fox LLP. J.N.O., F.B., and Q.W. work was supported by NSF (Grants PHY-2019745 and PHY-2019745) and by the Welch Foundation (Grant C-1792). J.N.O. is a CPRIT Scholar in Cancer Research sponsored by the Cancer Prevention and Research Institute of Texas.

Author affiliations: [a]Thoracic Oncology, University of Hawaii Cancer Center, Honolulu, HI 96813; [b]Center for Theoretical Biological Physics, Rice University, Houston, TX 77005; [c]Hefei National Laboratory for Physical Sciences at the Microscale and Department of Physics, University of Science and Technology of China, Hefei, Anhui 230026, China; [d]Department of Molecular Biosciences and Bioengineering, University of Hawaii at Manoa, Honolulu, HI 96822; [e]Shanghai Institute for Advanced Immunochemical Studies, ShanghaiTech University, Shanghai 201210, China; [f]School of Life Science and Technology, ShanghaiTech University, Shanghai 201210, China; [g]Department of Translational Medicine LTTA Centre University of Ferrara, Ferrara 44121, Italy; and [h]Department of Cardiothoracic Surgery, New York University, New York, NY 10016

Author contributions: J.N.O., H.Y., and M.C. designed research; A.B., Q.W., A.A.Z., F.B., M.S-T., J.S.S., S.P., A.S., V.S., A.F., F.N., J.-H.K., M.M., Y.T., L.P., A.N., R.X., C.F., C.G., G.S., G.G., and H.I.P. performed research; C.B., M.N., and I.P. analyzed data; G.S. and H.I.P. contributed surgical specimens; and A.B. and M.C. wrote the paper.

Reviewers: P.P.P., Renown Institute for Cancer; and I.L.P., Northwestern University.

Competing interest statement: The authors have organizational affiliations to disclose. M.C. is a board-certified pathologist who provides consultation for pleural pathology, including medical-legal. The authors have patent filings to disclose. M.C. has a patent issued for "Methods for Diagnosing a Predisposition to Develop Cancer".

1. M. Carbone *et al.*, Biological mechanisms and clinical significance of BAP1 mutations in human cancer. *Cancer Discov.* **10**, 1103–1120 (2020).
2. E. Conway *et al.*, BAP1 enhances polycomb repression by counteracting widespread H2AK119ub1 deposition and chromatin condensation. *Mol. Cell* **81**, 3526–3541.e8 (2021).
3. L. Masclef *et al.*, Roles and mechanisms of BAP1 deubiquitinase in tumor suppression. *Cell Death Differ.* **28**, 606–625 (2021).
4. A. Bononi *et al.*, BAP1 regulates IP3R3-mediated Ca(2+) flux to mitochondria suppressing cell transformation. *Nature* **546**, 549–553 (2017).
5. A. Bononi *et al.*, Germline BAP1 mutations induce a Warburg effect. *Cell Death Differ.* **24**, 1694–1704 (2017).
6. M. Carbone *et al.*, Medical and surgical care of patients with mesothelioma and their relatives carrying germline BAP1 mutations. *J. Thorac. Oncol.* **17**, 873–889 (2022), 10.1016/j.jtho.2022.03.014.
7. M. Carbone *et al.*, Combined genetic and genealogic studies uncover a large BAP1 cancer syndrome kindred tracing back nine generations to a common ancestor from the 1700s. *PLoS Genet.* **11**, e1005633 (2015).
8. J. R. Testa *et al.*, Germline BAP1 mutations predispose to malignant mesothelioma. *Nature Genet.* **43**, 1022–1025 (2011).
9. S. Walpole *et al.*, Comprehensive study of the clinical phenotype of germline BAP1 variant-carrying families Worldwide. *J. Natl Cancer Inst.* **110**, 1328–1341 (2018).
10. R. Bernardi *et al.*, PML inhibits HIF-1alpha translation and neoangiogenesis through repression of mTOR. *Nature* **442**, 779–785 (2006).
11. A. Bononi *et al.*, Heterozygous germline BLM mutations increase susceptibility to asbestos and mesothelioma. *Proc. Natl. Acad. Sci. U.S.A.* **117**, 33466–33473 (2020).
12. S. Pastorino *et al.*, A subset of mesotheliomas with improved survival occurring in carriers of BAP1 and other germline mutations. *J. Clin. Oncol.* **36**, JCO2018790352 (2018), 10.1200/JCO.2018.79.0352.
13. V. Panou *et al.*, Frequency of germline mutations in cancer susceptibility genes in malignant mesothelioma. *J. Clin. Oncol.* **36**, 2863–2871 (2018).
14. M. Carbone *et al.*, Tumour predisposition and cancer syndromes as models to study gene-environment interactions. *Nat. Rev. Cancer* **20**, 533–549 (2020).
15. S. Comertpay *et al.*, Evaluation of clonal origin of malignant mesothelioma. *J. Translat. Med.* **12**, 301 (2014).
16. M. Carbone *et al.*, Mesothelioma: Scientific clues for prevention, diagnosis, and therapy. *CA Cancer J. Clin.* **69**, 402–429 (2019).
17. A. S. Tsao *et al.*, Current and future management of malignant mesothelioma: A consensus report from the national cancer institute thoracic malignancy steering committee, international association for the study of lung cancer, and mesothelioma applied research foundation. *J. Thorac. Oncol.* **13**, 1655–1667 (2018).
18. L. Mutti *et al.*, Scientific advances and new frontiers in mesothelioma therapeutics. *J. Thorac. Oncol.* **13**, 1269–1283 (2018).
19. H. Yang *et al.*, Aspirin delays mesothelioma growth by inhibiting HMGB1-mediated tumor progression. *Cell Death Dis.* **6**, e1786 (2015).
20. Z. Rivera *et al.*, CSPG4 as a target of antibody-based immunotherapy for malignant mesothelioma. *Clin. Cancer Res.* **18**, 5352–5363 (2012).
21. C. M. Goparaju *et al.*, Onconase mediated NFKβ downregulation in malignant pleural mesothelioma. *Oncogene* **30**, 2767–2777 (2011).
22. M. Nasu *et al.*, Ranpirnase interferes with NF-κB pathway and MMP9 activity, inhibiting malignant mesothelioma cell invasiveness and xenograft growth. *Genes Cancer* **2**, 576–584 (2011).
23. H. I. Pass *et al.*, Inhibition of hamster mesothelioma tumorigenesis by an antisense expression plasmid to the insulin-like growth factor-1 receptor. *Cancer Res.* **56**, 4044–4048 (1996).
24. D. B. Chapel, J. J. Schulte, A. N. Husain, T. Krausz, Application of immunohistochemistry in diagnosis and management of malignant mesothelioma. *Transl. Lung Cancer Res.* **9**, S3–S27 (2020).
25. M. Farzin *et al.*, Loss of expression of BAP1 predicts longer survival in mesothelioma. *Pathology* **47**, 302–307 (2015).
26. A. Louw *et al.*, BAP1 loss by immunohistochemistry predicts improved survival to first-line platinum and pemetrexed chemotherapy for patients with pleural mesothelioma: A validation study. *J. Thorac. Oncol.* **17**, 921–930 (2022).
27. F. Baumann *et al.*, Mesothelioma patients with germline BAP1 mutations have 7-fold improved long-term survival. *Carcinogenesis* **36**, 76–81 (2015).
28. R. Hassan *et al.*, Inherited predisposition to malignant mesothelioma and overall survival following platinum chemotherapy. *Proc. Natl. Acad. Sci. U.S.A.* **116**, 9008–9013 (2019).
29. R. M. Flores *et al.*, Extrapleural pneumonectomy versus pleurectomy/decortication in the surgical management of malignant pleural mesothelioma: Results in 663 patients. *J. Thorac. Cardiovasc. Surg.* **135**, 620–626 (2008), 626.e1-3.
30. E. Moroz *et al.*, Real-time imaging of HIF-1alpha stabilization and degradation. *PLoS One* **4**, e5077 (2009).
31. N. Ferrara, T. Davis-Smyth, The biology of vascular endothelial growth factor. *Endocr. Rev.* **18**, 4–25 (1997).
32. P. Cacciotti *et al.*, SV40 replication in human mesothelial cells induces HGF/Met receptor activation: A model for viral-related carcinogenesis of human malignant mesothelioma. *Proc. Natl. Acad. Sci. U.S.A.* **98**, 12032–12037 (2001).
33. M. S. Nakazawa, B. Keith, M. C. Simon, Oxygen availability and metabolic adaptations. *Nat. Rev. Cancer* **16**, 663–673 (2016).
34. G. L. Semenza, HIF-1 mediates metabolic responses to intratumoral hypoxia and oncogenic mutations. *J. Clin. Invest.* **123**, 3664–3671 (2013).
35. M. Nasu *et al.*, High incidence of somatic BAP1 alterations in sporadic malignant mesothelioma. *J. Thorac. Oncol.* **10**, 565–576 (2015).
36. R. Bueno *et al.*, Comprehensive genomic analysis of malignant pleural mesothelioma identifies recurrent mutations, gene fusions and splicing alterations. *Nat. Genet.* **48**, 407–416 (2016).
37. D. E. Jensen *et al.*, BAP1: A novel ubiquitin hydrolase which binds to the BRCA1 RING finger and enhances BRCA1-mediated cell growth suppression. *Oncogene* **16**, 1097–1112 (1998).
38. A. Davtyan *et al.*, AWSEM-MD: Protein structure prediction using coarse-grained physical potentials and bioinformatically based local structure biasing. *J. Phys. Chem. B* **116**, 8494–8503 (2012).
39. A. Roy, A. Kucukural, Y. Zhang, I-TASSER: A unified platform for automated protein structure and function prediction. *Nat. Protoc.* **5**, 725–738 (2010).
40. J. Yang *et al.*, The I-TASSER Suite: Protein structure and function prediction. *Nat. Methods* **12**, 7–8 (2015).
41. J. Yang, Y. Zhang, I-TASSER server: New development for protein structure and function predictions. *Nucleic Acids Re.s* **43**, W174–W181 (2015).
42. M. Kallberg *et al.*, Template-based protein structure modeling using the RaptorX web server. *Nat. Protoc.* **7**, 1511–1522 (2012).
43. S. Vajda *et al.*, New additions to the ClusPro server motivated by CAPRI. *Proteins* **85**, 435–444 (2017).
44. D. Kozakov *et al.*, The ClusPro web server for protein-protein docking. *Nat. Protoc.* **12**, 255–278 (2017).
45. D. Kozakov *et al.*, How good is automated protein docking? *Proteins* **81**, 2159–2166 (2013).
46. S. Wang, S. Sun, Z. Li, R. Zhang, J. Xu, Accurate de novo prediction of protein contact map by ultra-deep learning model. *PLoS Comput. Biol.* **13**, e1005324 (2017).
47. B. A. Shoemaker, J. J. Portman, P. G. Wolynes, Speeding molecular recognition by using the folding funnel: The fly-casting mechanism. *Proc. Natl. Acad. Sci. U.S.A.* **97**, 8868–8873 (2000).
48. E. Trizac, Y. Levy, P. G. Wolynes, Capillarity theory for the fly-casting mechanism. *Proc. Natl. Acad. Sci. U.S.A.* **107**, 2746–2750 (2010).
49. D. Wu, N. Potluri, J. Lu, Y. Kim, F. Rastinejad, Structural integration in hypoxia-inducible factors. *Nature* **524**, 303–308 (2015).
50. A. Waterhouse *et al.*, SWISS-MODEL: Homology modelling of protein structures and complexes. *Nucleic Acids Res.* **46**, W296–W303 (2018).
51. L. E. Huang, J. Gu, M. Schau, H. F. Bunn, Regulation of hypoxia-inducible factor 1alpha is mediated by an O2-dependent degradation domain via the ubiquitin-proteasome pathway. *Proc. Natl. Acad. Sci. U.S.A.* **95**, 7987–7992 (1998).
52. G. L. Semenza, HIF-1 and mechanisms of hypoxia sensing. *Curr. Opin. Cell Biol.* **13**, 167–171 (2001).
53. G. L. Semenza, A compendium of proteins that interact with HIF-1alpha. *Exp. Cell Res.* **356**, 128–135 (2017).
54. Y. Goto *et al.*, UCHL1 provides diagnostic and antimetastatic strategies due to its deubiquitinating effect on HIF-1alpha. *Nat. Commun.* **6**, 6153 (2015).
55. P. Hanpude, S. Bhattacharya, A. Kumar Singh, T. Kanti Maiti, Ubiquitin recognition of BAP1: Understanding its enzymatic function. *Biosci. Rep.* **37**, BSR20171099 (2017).
56. J. C. Scheuermann *et al.*, Histone H2A deubiquitinase activity of the polycomb repressive complex PR-DUB. *Nature* **465**, 243–247 (2010).
57. R. Zarrizi, J. A. Menard, M. Belting, R. Massoumi, Deubiquitination of gamma-tubulin by BAP1 prevents chromosome instability in breast cancer cells. *Cancer Res.* **74**, 6499–6508 (2014).
58. E. J. Yeo *et al.*, YC-1: A potential anticancer drug targeting hypoxia-inducible factor 1. *J. Natl. Cancer Inst.* **95**, 516–525 (2003).
59. T. Shukuya *et al.*, Hypoxia inducible factor-1alpha Inhibition in Von Hippel Lindau-mutant malignant pleural mesothelioma cells. *Anticancer Res.* **40**, 1867–1874 (2020).
60. R. J. Francis *et al.*, Characterization of hypoxia in malignant pleural mesothelioma with FMISO PET-CT. *Lung Cancer* **90**, 55–60 (2015).
61. N. J. Brouwer *et al.*, Ischemia is related to tumour genetics in uveal melanoma. *Cancers (Basel)* **11**, 1004 (2019).
62. S. S. Wang *et al.*, Bap1 is essential for kidney function and cooperates with Vhl in renal tumorigenesis. *Proc. Natl. Acad. Sci. U.S.A.* **111**, 16538–16543 (2014).
63. Y. F. Gu *et al.*, Modeling renal cell carcinoma in mice: Bap1 and Pbrm1 inactivation drive tumor grade. *Cancer Discov.* **7**, 900–917 (2017).
64. T. J. Mitchell *et al.*, Timing the landmark events in the evolution of clear cell renal cell cancer: TRACERx renal. *Cell* **173**, 611–623.e17 (2018).
65. J. W. Harbour *et al.*, Frequent mutation of BAP1 in metastasizing uveal melanomas. *Science.* **330**, 1410–1413 (2010).
66. Y. Yoshikawa *et al.*, High-density array-CGH with targeted NGS unmask multiple noncontiguous minute deletions on chromosome 3p21 in mesothelioma. *Proc. Natl. Acad. Sci. U.S.A.* **113**, 13432–13437 (2016).